Systematic and Facile Analysis of Deposits Composition: Implication on Effective Treatment of Oilfield Solid Deposits

Emanuel X. Ricky
Key Laboratory of Theory and Technology of Petroleum Exploration and Development in Hubei Province,
China University of Geosciences,
Wuhan 430074, China;
Key Laboratory of Tectonics and Petroleum Resources Ministry of Education,
China University of Geosciences,
Wuhan 430074, China;
Department of Chemistry,
College of Natural and Applied Sciences,
University of Dar es Salaam,
P. O. Box 35061,
Dar es Salaam, Tanzania
e-mail: ricky.emanuel@udsm.ac.tz

Xingguang Xu[1]
Key Laboratory of Theory and Technology of Petroleum Exploration and Development in Hubei Province,
China University of Geosciences,
Wuhan 430074, China;
Key Laboratory of Tectonics and Petroleum Resources Ministry of Education,
China University of Geosciences,
Wuhan 430074, China
email: xuxingguang@cug.edu.cn

Oilfield solid deposits present the major flow assurance problems in the oil and gas industry. In general, the deposits need to be accurately identified and quantified for appropriate design and successful implementation of any treatments. However, few works have been reported on the establishment of a systematic analytical procedure. This work, for the first time, presents a systematic approach that may be used to identify and quantify the composition of oilfield solid deposits, with different analytical methods been jointly used. The X-ray diffraction (XRD) and Fourier transform infrared (FT-IR) spectroscopy techniques were found very helpful in identifying the composition of the investigated oilfield solid deposit, whereas thermogravimetric analysis (TGA) and microwave induced plasma atomic emission spectroscopy (MIP-AES) were the most appropriate quantification techniques. The collected sample was found to contain mainly $CaCO_3$ and consequently, the acid treatment method that involves the use of hydrochloric acid (HCl) solution was proposed to be the most applicable and cost-effective treatment method for its remediation. The exact amount of $CaCO_3$ scale in the oilfield system, the concentration and volume of HCl solution required for the acid treatment method need to be precisely determined to ensure the effective treatment. We believe this well-established analytical procedure will be helpful and enlightening for identification and quantification of oilfield solid deposits and thus may facilitate the effective and efficient treatments on the undesirable deposits.
[DOI: 10.1115/1.4051897]

Keywords: oilfield solid deposit, qualitative analysis, quantitative analysis, flow assurance problem, treatment, petroleum engineering, petroleum transport/pipelines/multiphase flow, petroleum wells-drilling/production/construction

Introduction

Solid deposits in the oilfield systems may include wax, paraffin, gas hydrates, asphaltenes, naphthenates, and mineral scales [1–6]. Oilfield solids deposition in the oilfield systems usually occurs in the reservoirs, wellbores, well casings, separators, pipelines, heat exchangers, and storage tanks [2,4,7–9]. The oilfield solid deposits are grouped mainly into organic and inorganic. Organic solid deposits are mainly due to the formation of wax, paraffin, asphaltenes, naphthenates, and gas hydrates [3,6,10]. Inorganic solid deposits are mainly due to the formation of mineral scales such as $CaCO_3$, $CaSO_4$, $BaSO_4$, $SrSO_4$, $MgCO_3$, FeS, and $FeCO_3$ [11,12].

The main driving forces for the formation of oilfield solid deposits in the oilfield systems include changes in temperature, pressure, pH, and mixing of two incompatible fluids [10,13,14]. Wax and paraffin deposition is influenced by the changes in temperature and/or pressure in the oilfield systems [15–17]. However, the formation of wax crystals is much influenced by the temperature drop, especially in the subsea oil and gas pipelines [15,17,18]. Gas hydrates are formed in the oil and gas production systems when gases such as methane, ethane, propane, carbon dioxide, and hydrogen sulfide react with water at low temperatures and high pressure [16,19,20]. Asphaltene deposition usually occurs in the downstream production systems due to changes in temperature and/or pressure [21,22].

The most commonly encountered oilfield solid deposits in the oilfield systems are mineral scale deposits due to carbonate and sulfate scale depositions [13,23]. Carbonate scales such as $CaCO_3$, $MgCO_3$, and $FeCO_3$ occur in the oil and gas production systems mainly due to changes in temperature and/or pressure [2,11,24]. In most cases when the temperature of the brine solution in the production systems increases, the bicarbonate salts become unstable and decomposes to CO_2 and $CaCO_3$ [7,24]. Using $CaCO_3$ as an example, the chemistry of carbonate scales formation from an aqueous solution of bicarbonate salt is shown in Eq. (1) [23]

$$Ca(HCO_3)_2(aq) \underset{\Delta}{\rightleftharpoons} CO_2(g) + H_2O(g) + CaCO_3(s) \quad (1)$$

The precipitation of $CaCO_3$ is favored by a decrease in CO_2 partial pressure and an increase in temperature of the brine solution in the oil and gas production systems [7,25]. Apart from temperature and pressure, the formation of carbonate scales is also influenced by other factors such as carbonic acid concentration (Eq. (2)), pH (Eq. (3)), metal, and bicarbonate ions concentration (Eq. (4)) [2,4,12,14,25]

$$CO_2(aq) + H_2O(I) \rightleftharpoons H_2CO_3(aq) \quad (2)$$

$$H_2CO_3(aq) \rightleftharpoons 2H^+(aq) + CO_3^{2-}(aq) \quad (3)$$

$$Ca^{2+}(aq) + CO_3^{2-}(aq) \rightleftharpoons CaCO_3(s) \quad (4)$$

[1]Corresponding author.

Contributed by the Petroleum Division of ASME for publication in the Journal of Energy Resources Technology. Manuscript received February 2, 2021; final manuscript received July 15, 2021; published online August 11, 2021. Assoc. Editor: Ray (Zhenhua) Rui.

Sulfate scales mainly $BaSO_4$, $SrSO_4$, and $CaSO_4$ are formed in the oil and gas production systems due to the mixing of two incompatible brine solutions [24,26,27]. During secondary oil and gas recovery, seawater is injected into the reservoir to maintain the pressure of the reservoir, and to improve the oil and gas recovery efficiency. Seawater contains dissolved anions mainly SO_4^{2-}, HCO_3^-, and Cl^- while the reservoir formations are rich in cations such as Ca^{2+}, Ba^{2+}, Sr^{2+}, Fe^{2+}, Mg^{2+}, and Na [7,26]. Thus, the injection of seawater with SO_4^{2-} into the reservoir formation rich in Ca^{2+}, Ba^{2+}, and Sr^{2+} results in precipitation of $CaSO_4$, $BaSO_4$, and $SrSO_4$ scales as shown in Eq. (5) [2,12,24]

$$Ba^{2+}\text{ or }Ca^{2+}\text{ or }Sr^{2+}\text{ (aq)} + SO_4^{2-}\text{(aq)} \rightleftharpoons BaSO_4\text{ or }CaSO_4\text{ or }SrSO_4\text{(s)} \quad (5)$$

Both organic and inorganic oilfield solid deposits cause flow assurance problems in the oil and gas production systems by interfering with the flow of hydrocarbon streams from the reservoir to the point of sale or processing unit [28]. Oilfield solid deposits can block the oil and gas pipelines, processing equipment, wellbore, and formation fractures in the reservoirs [7,13,21,26,29,30]. Several case studies have been reported based on the deposition of oilfield solid materials in the oil and gas production systems including the gas hydrate deposition plug in the subsea pipeline of Petrobras in Brazil [31]; wax deposition plug in the Kirkuk-Ceyhan crude oil pipeline between Iraq and Turkey, Power Play oil pipeline in the Gulf of Mexico and subsea oil pipeline of Gannet in Aberdeen (UK) [15], and $CaCO_3$ scale deposition in production and transportation equipment [32,33]. Figure 1 shows the flow assurance problems due to the deposition of oilfield solid materials such as wax, hydrates, and $CaCO_3$ scale in the oil and gas pipelines from different areas.

Generally, the deposition of oilfield solid materials in the oil and gas production systems can result in fluid flow restriction, failure of production equipment, decreased porosity and permeability of the reservoir formation, and increased maintenance and production cost [7,13,29]. Therefore, the flow assurance problems due to oilfield solid deposits need to be properly addressed to maintain a continuous flow of hydrocarbons at the required flowrates from the reservoir to the point of sale and to reduce the production and maintenance costs [23].

Various preventive methods have been used in the oil and gas industry to overcome the flow assurance problems due to oilfield solid deposits. These include thermal insulation of pipelines to control the temperature, injection of chemical inhibitors to inhibit the formation of oilfield solid deposits, and the use of reverse osmosis or adsorbent materials to remove dissolved mineral ions from seawater during water flooding in secondary oil and gas recovery [27,34]. Once the oilfield solid deposits are formed in the oil and gas production systems, some remediation methods, namely, mechanical and chemical treatment methods can be used to remove the deposits. Mechanical treatment methods include scraping, drilling, brushing, and milling while chemical treatment methods involve the use of hydrochloric acid (HCl), hydrofluoric acid (HF), acetic acid, citric acid, formic acid, and chelating agents such as ethylenediaminetetraacetic acid (EDTA) [2,13,29,34].

Chemical treatment methods are the most favorable techniques when dealing with oilfield solid deposits where other methods are infeasible [13,29]. The effectiveness of the chemical treatment method is reliant on the chemical composition and quantity of oilfield solid deposits. The chemistry and quantity of oilfield solid deposits are imperative factors in the selection of the most appropriate and cost-effective chemical treatment method. The oilfield solid deposits need to be identified and quantified first for better designing of the most appropriate and cost-effective treatment method. However, the biggest challenge when dealing with unknown oilfield solid deposits is how to go about; which analytical methods should be used to identify and quantify the unknown oilfield solid deposits. This challenge can only be handled through the application of analytical procedures that involve the use of qualitative and quantitative analysis. The qualitative analysis helps to identify what analytes are present in the given unknown oilfield samples whereas the quantitative analysis helps to determine how much analytes are present in the given unknown oilfield samples. The qualitative analysis provides an insight into the problem and helps to develop hypotheses for the quantitative analysis [35]. Quantitative analysis helps to quantify the analytes present in the given unknown oilfield samples by generating numerical data.

Since the oilfield solid deposits present the major flow assurance problems in the oil and gas industry. The results obtained from the qualitative and quantitative analysis of oilfield solid deposits are very useful in designing the most appropriate and cost-effective treatment method. However, to the best of our knowledge, there are a few research works that have been done on oilfield samples and there is limited information regarding the analysis and treatment of unknown oilfield solid deposits. Therefore, there is a need for establishing analytical procedures for identifying and quantifying the unknown oilfield solid deposits, henceforth selecting the appropriate treatment method. Thus, this study briefly presents a systematic approach for the qualitative and quantitative analysis, and treatment of oilfield solid deposits using an unknown oilfield solid deposit collected from an oilfield. A well-established analytical procedure for the identification and quantification of unknown oilfield solid deposits can help to reduce the guesswork in the due course of analysis. The proper selection of the analytical methods and the most appropriate treatment method for the unknown oilfield solid deposits can save money and time for the analysis which is the ultimate goal of the oil and gas industry.

Experimental Section

Materials. An unknown oilfield solid deposit labelled sample "E" was collected from an oilfield. The chemicals used in this study include HCl (37%), nitric acid (HNO_3) (68%), calcium carbonate ($CaCO_3$) (99%), iron(III) nitrate nonahydrate ($Fe(NO_3)_3 \cdot 9H_2O$) (98.8%), magnesium sulfate ($MgSO_4$) (98%), copper

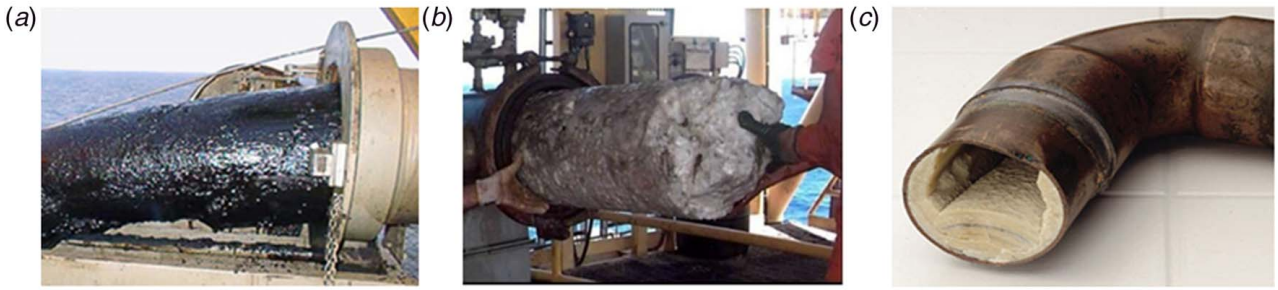

Fig. 1 Solid deposits due to (*a*) wax plug [15], (*b*) hydrate plug [31], and (*c*) $CaCO_3$ scale [32]

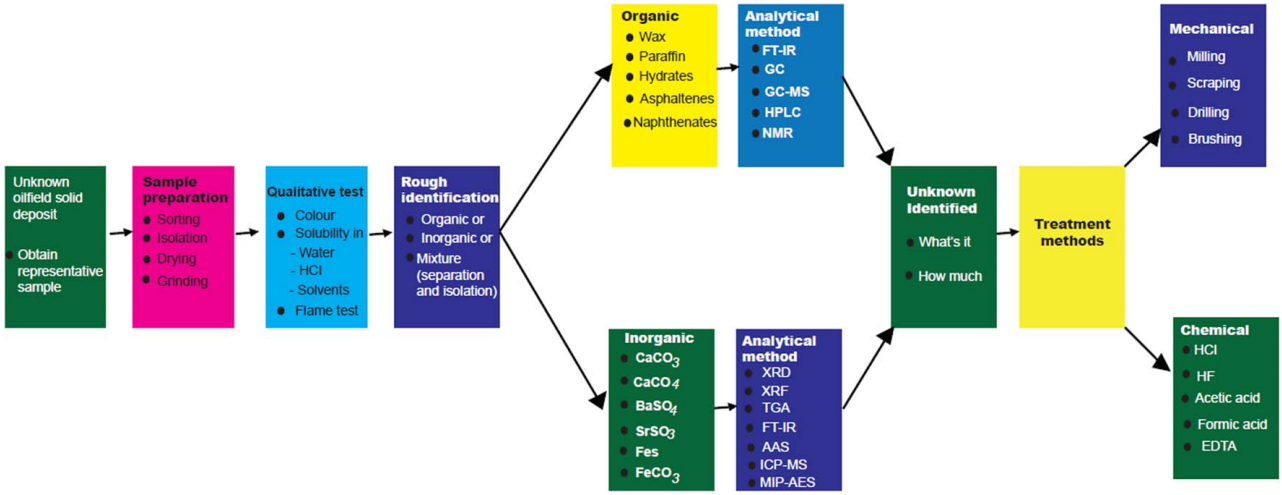

Fig. 2 General schematic approach for the identification, quantification, and treatment of unknown oilfield solid deposits

sulfate pentahydrate ($CuSO_4 \cdot 5H_2O$) (98%), barium carbonate ($BaCO_3$) (98%), sodium sulfate (Na_2SO_4) (99%), strontium nitrate ($Sr(NO_3)_2$) (99%), and double deionized water. All the chemicals used in this study were purchased from Sigma Aldrich and they were used as supplied.

Methodology. The choice of which analytical methods are suitable for the identification and quantification of an unknown oilfield solid deposit is one of the most difficult parts of the analysis. In the present study, some preliminary qualitative tests such as flame test and solubility (in water, mineral acids, and organic solvents) were carried out prior to analytical measurements to identify roughly whether the unknown oilfield solid deposit sample E is an organic or inorganic solid deposit. The selection of the appropriate analytical methods for the identification and quantification of unknown oilfield solid deposit sample E was accomplished following the approach shown in Fig. 2.

Preliminary Qualitative Test. The unknown oilfield solid deposit sample E was a hard-gray solid particle. A representative fraction of sample E was ground into fine powder by using mortar and pestle. Some preliminary qualitative tests such as flame test and solubility (in water, 15% HCl solution, toluene, and n-hexane) were conducted to identify roughly whether the unknown oilfield solid deposit sample E is an organic or inorganic solid deposit. A small amount of solid particle sample E was subjected to a flame source; subsequently, 1 g of fine powdered sample E was dissolved in 5 mL of double deionized water, 15% HCl solution, toluene, and n-hexane, respectively. Based on the findings from the preliminary qualitative tests and the available instruments, X-ray diffraction (XRD), thermogravimetric analysis (TGA), Fourier transform infrared (FT-IR), and microwave induced plasma atomic emission spectrometry (MIP-AES) were chosen for the identification and quantification of the unknown oilfield solid deposit sample E.

X-Ray Diffraction Analysis. This technique is commonly used in the oil and gas industry for the identification of mineral phases present in oilfield samples. In this study, a small amount of solid deposit sample E was ground into fine powder by using mortar and pestle. The finely powdered sample was then placed in a stainless-steel sample holder and smeared uniformly with a glass slide to obtain a uniform upper surface. The sample holder was placed into a sample holder container and analyzed by X-ray Powder Diffractometer (Panalytical X-Pert) using Cu-Kα radiation in the range of 2θ between 10 deg and 80 deg.

Thermogravimetric Analysis. This method is commonly used for the quantitative analysis of oilfield samples, in the present study the analysis was carried out to determine the weight loss fraction of sample E as a function of temperature on heating. A small amount of solid deposit sample E was ground into fine powder by using mortar and pestle. Then, 42.230 mg of fine powdered sample E was placed in a sample holder and analyzed by Thermogravimetric Analyzer (Mettler Toledo/Balzers, TGA2/ThermoStar) at a heating rate of 10 °C/min over a range of 25–1000 °C.

Fourier Transform Infrared Analysis. This technique was used to identify whether the unknown oilfield solid deposit sample E was an organic or inorganic solid deposit. FT-IR analysis of sample E was conducted to obtain information about the functional groups of chemical constituents present in the unknown oilfield solid deposit sample E. A small amount of solid deposit sample E was ground into fine powder by using mortar and pestle. Then a small amount of finely powdered sample E was placed on the ATR diamond disc and scanned over a range of 4000–400 cm^{-1} by FT-IR spectrometer (Perkin-Elmer, Spectrum Version10.4.00) to obtain the FT-IR spectrum.

Microwave Induced Plasma-Atomic Emission Spectrometry Analysis. This technique was used to determine the elemental composition of sample E. An aqua regia solution was prepared by mixing 75 mL and 25 mL of concentrated HCl and HNO_3, respectively, in a 250 mL beaker. The acid digestion of sample E was carried out as reported elsewhere [36]. The filtrate solution obtained from the acid digestion was analyzed by MIP-AES (MP4200 Agilent) for the general elemental scan to identify all the elements present in oilfield solid deposit sample E. From the general elemental scan by MIP-AES, the emission intensity of Ca in the filtrate solution was found to be very high as compared with other elements, this implies that its concentration in sample E is also very high as compared with other elements. Thus, its quantification was done separately by using 0.0151 g of sample E with some dilution whereas for other elements 0.2 g of sample E was used. After the general elemental scan by MIP-AES, different standard solutions were prepared to make a stock solution of multi-element from which the working solutions were prepared as reported in the "Preparation of Working Solutions" section.

Preparation of 1000 ppm Standard Solutions. Standard (Std) solutions were prepared for the quantification of each element (Ca, Na, Mg, Fe, Ba, Sr, and Cu) found in unknown solid deposit sample E based on the general elemental scan results by MIP-AES.

Table 1 Preparation of 1000 ppm standard solutions

Salt used	Molar mass of salt (g/mol)	Mass of salt used (g)	Element of interest	Std solution (ppm)
$CaCO_3$	100.09	2.4972	Ca	1000
$Fe(NO_3)_3 \cdot 9H_2O$	404.00	7.2344	Fe	1000
$MgSO_4$	120.37	4.9522	Mg	1000
$CuSO_4 \cdot 5H_2O$	249.68	3.9291	Cu	1000
$BaCO_3$	197.35	1.4370	Ba	1000
Na_2SO_4	142.04	6.1785	Na	1000
$Sr(NO_3)_2$	211.63	2.4152	Sr	1000

1000 ppm standard solutions of Ca, Na, Mg, Fe, Ba, Sr, and Cu were prepared as shown in Table 1. The mass of each salt used to prepare the 1000 ppm standard solution of each element was calculated and reported in Table 1.

Preparation of Multi-Element Standard Solution. Since MIP-AES offers simultaneous multi-element analysis, a stock solution of 50 ppm multi-element standard solution was prepared by mixing 25 mL of each 1000 ppm standard solution of Ca, Na, Mg, Fe, Ba, Sr, and Cu in 500 mL volumetric flask and diluted to the mark with double deionized water.

Preparation of Working Solutions. Different working solutions were prepared from the multi-element standard solution as illustrated in Table 2. Finally, the prepared standard working solutions and the solution of unknown oilfield solid deposit sample E were analyzed by MIP-AES.

Acid Dissolving Power. Upon the identification of unknown oilfield solid deposit sample E as $CaCO_3$, the acid treatment method that involves the use of HCl solution was proposed to be the most appropriate treatment method for the removal of solid deposit sample E. The acid dissolving power was determined by dissolving 3.001 g of sample E in different volumes (1, 3, 5, 7, 9, 11, 13, and 15 mL) of 15% HCl solution in different 100 mL beakers at room temperature for 30 min. After 30 min, the mixtures were filtered using Whatman filter papers and the residuals obtained were washed with double deionized water and allowed to dry at room temperature for 12 h. The residuals were then weighed, the change in mass was calculated and the acid dissolving power was determined from the weight loss.

Results and Discussion

Preliminary Qualitative Test. In the current study, some preliminary qualitative tests were conducted prior to analytical measurements for better selection of appropriate analytical methods for the identification and quantification of unknown oilfield solid deposit sample E. From the preliminary qualitative tests conducted, it was observed that the unknown oilfield solid deposit sample E was gray, insoluble (in water, toluene, and n-hexane) and did not burn on flame; but it was soluble in 15% HCl giving out an effervescence probably due to the evolution of CO_2 gas. This indicated that the unknown oilfield solid deposit sample E was likely to be inorganic carbonate scale deposits. Thus, based on the available instruments; XRD, TGA, FT-IR, and MIP-AES were chosen for its identification and quantification.

Table 2 Preparation of working solutions from the multi-element standard solution

Volume of multi-element stock solution taken (mL)	Total volume of working solution (mL)	Concentration of working solution (ppm)
1	100	0.50
10	100	5.00
20	100	10.0
30	100	15.0
40	100	20.0
50	100	25.0

The following are the general observations on a preliminary qualitative test of oilfield solid deposits; *color*: most organic solid deposits are usually black due to the presence of carbon residues while inorganic solid deposits are either gray, off-white, brown, or greenish. *Flame test*: organic solid deposits burns when subjected to a flame source producing soot and leaving behind black carbon residues, while the inorganic scale deposits do not burn on flame but can only form ash when subjected to a very high temperature. *Solubility test*: inorganic mineral scales are insoluble in water except for NaCl; likewise, organic solid deposits are insoluble in water except those with many oxygen atoms or OH functional groups in their structures. Most of the inorganic mineral scales except $BaSO_4$ and $SrSO_4$ are soluble or slightly soluble in mineral acids such as HCl and HNO_3 whereas organic solid deposits are insoluble. On the other hand, organic solid deposits are soluble in some organic solvents; for example, asphaltenes are soluble in toluene but insoluble in n-hexane while wax and gas hydrates are soluble in n-hexane. Inorganic mineral scales are insoluble in organic solvents. These general observations are made from our research experiences in dealing with the oilfield samples and basic understanding of qualitative analysis.

X-Ray Diffraction Analysis. The XRD analysis was carried out to identify the mineral phases present in unknown oilfield solid deposit sample E. Figure 3 shows the diffractogram of unknown solid deposit sample E, the results revealed that the unknown solid deposit sample E was aragonite ($CaCO_3$). The diffractogram showed the presence of characteristic peaks of aragonite with a distinctive prominent inter-atomic d-spacing of 3.396 Å, 3.273 Å, 2.700 Å, and 1.977 Å at 2θ value of 26 deg, 27 deg, 33 deg, and 46 deg, respectively. The obtained diffractogram of aragonite was overlaid with the diffractogram of aragonite standard reference material (International Center for Diffraction Data (ICDD) 00-024-0025) from the computer database. The two diffractograms have shown a perfect match indicating that the unknown solid deposit sample E was aragonite ($CaCO_3$). Similar observations were also reported by Xu and Poduska [37] on the study of crystallinity differences and temperature dependency of carbonate minerals by XRD. Sarkar and Mahapatra [38] have also reported a similar XRD diffractogram

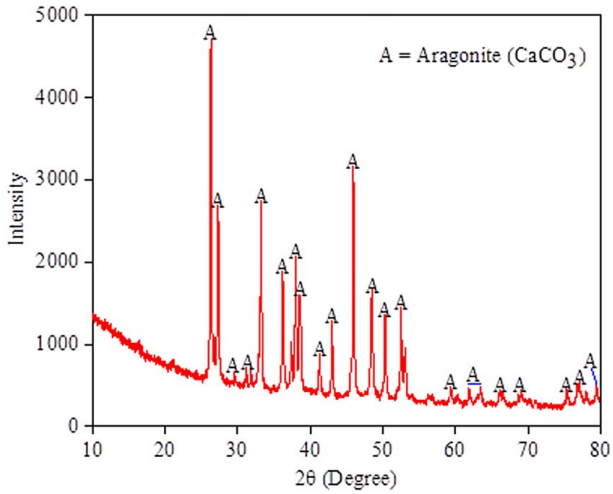

Fig. 3 XRD diffractogram pattern of unknown solid deposit sample E

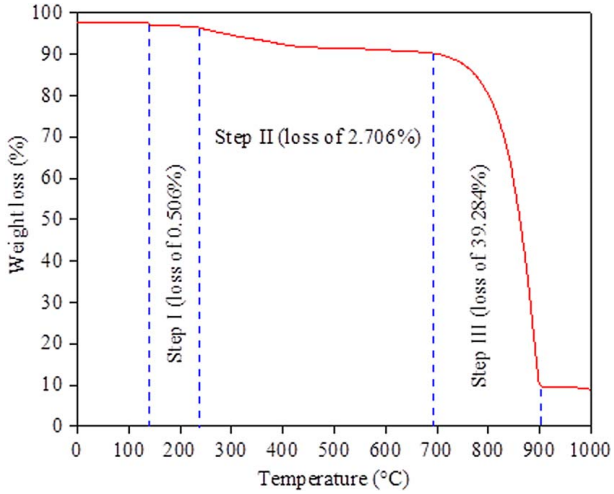

Fig. 4 TGA curve for the decomposition of unknown solid deposit sample E

of aragonite from unusual polymorph transformations of calcium carbonate. Thus, based on these findings, XRD is recommended as a powerful technique for the identification of unknown oilfield solid deposits especially inorganic mineral scale deposits.

Thermogravimetric Analysis. The weight loss of unknown oilfield solid deposit sample E was recorded as a function of temperature change. From the results obtained, three weight loss fractions were observed at different temperature ranges as shown in the TGA profile of the solid deposit sample E (Fig. 4); these ranges are defined as steps I, II, and III. The weight loss fraction at each temperature range and the associated process are summarized in Table 3.

The total weight loss observed in all three steps is 42.496%; this meant that 57.504% of the solid deposit sample E was undecomposable and was presumed to be calcium oxide (CaO). The decomposition reaction of $CaCO_3$ produces calcium oxide (CaO) and carbon dioxide CO_2 as shown in Eq. (6). The percentage weight loss of 39.284% (presumably CO_2) obtained from the TGA curve was used to calculate the percentage composition of $CaCO_3$ in the unknown oilfield solid deposit sample E with the aid of Eq. (6)

$$\underset{100.09\,g/mol}{CaCO_3(s)} \longrightarrow \underset{56.08\,g/mol}{CaO(s)} + \underset{44\,g/mol}{CO_2(g)} \quad (6)$$

The calculated percentage composition of the $CaCO_3$ scale in the unknown oilfield solid deposit sample E was found to be 89%. This implies that the unknown oilfield solid deposit sample E mainly composed of the $CaCO_3$ scale and these findings are in good agreement with the results obtained from XRD analysis. Similar results were also reported by Kodel et al. on the composition of mineral scales in oil wells by TGA [39]. Thus, this implies that TGA is a suitable method to quantify mineral scale deposits which exhibit distinctive decomposition characteristics.

Table 3 TGA results of oilfield solid deposit sample E

Step	Temperature interval (°C)	Weight loss fraction (%)	Process
I	100–200	0.506	Release of free or physically adsorbed water
II	300–600	2.706	Dehydration of hydrated crystal phases of sample E
III	700–900	39.284	Release of CO_2 through decomposition of sample E

Fourier Transform Infrared Analysis. Fourier transform infrared is very useful in the oil and gas industry in identifying organic and inorganic oilfield solid deposits. It gives information about the functional groups present in the oilfield solid deposits and can differentiate organic oilfield solid deposits from inorganic oilfield solid deposits. In most cases, inorganic oilfield solid deposits show their absorption bands in the fingerprint region (1500–400 cm^{-1}) while organic oilfield solid deposits are mainly characterized by the presence of a C-H bond with absorption bands at around 2800–3100 cm^{-1}. Figure 5 shows the FT-IR spectrum of unknown oilfield solid deposit sample E. The spectrum shows the absorption bands at 1455, 1082, 854, and 713 cm^{-1} as the characteristic absorption peaks of the carbonates functional group. Since each compound produces unique absorption peaks in the fingerprint region of the FT-IR spectrum. The absorption peaks at 1082, 854, and 713 cm^{-1} are unique to aragonite ($CaCO_3$), hence this indicated that aragonite was the major form of $CaCO_3$ in the unknown oilfield solid deposit sample E; thus, these results support the results obtained from XRD and TGA. Similar observations have also been reported by Xyla and Koutsoukos [40] on the quantitative analysis of calcium carbonate polymorphs by FT-IR.

Microwave Induced Plasma Atomic Emission Spectroscopy Analysis. This technique is not very famous in the oil and gas industry, it serves as an alternative technique to atomic absorption spectroscopy (AAS), inductively coupled plasma optical emission spectrometry (ICP-OES), inductively coupled plasma atomic emission spectrometry (ICP-AES), and inductively coupled plasma mass spectrometry (ICP-MS) for trace elemental analysis in oilfield samples [41–43]. It offers a fast and simultaneous multi-element analysis of oilfield samples as compared with AAS which can only analyze one element at a time per sample. However, ICP-OES, ICP-AES, and ICP-MS are the best techniques for the elemental analysis in oilfield samples than MIP-AES in terms of sensitivity, accuracy and detection limit, but they are not commonly used for the routine analysis in the oil and gas industry because of their high running costs as compared with MIP-AES [41]. The experimental results for the elemental analysis of unknown oilfield solid deposit sample E by MIP-AES for the detected elements (Ca, Ba, Sr, Na, Fe, Mg, and Cu) are shown in Table 4. The concentration of the detected elements was deduced from the calibration graph of each element.

The results presented in Table 4 are in the mean of triplicate measurements with RSD less than 10% which is acceptable as an experimental error for the concentration reported in ppm [41]. The actual concentration in weight per cent (wt%) of each element in

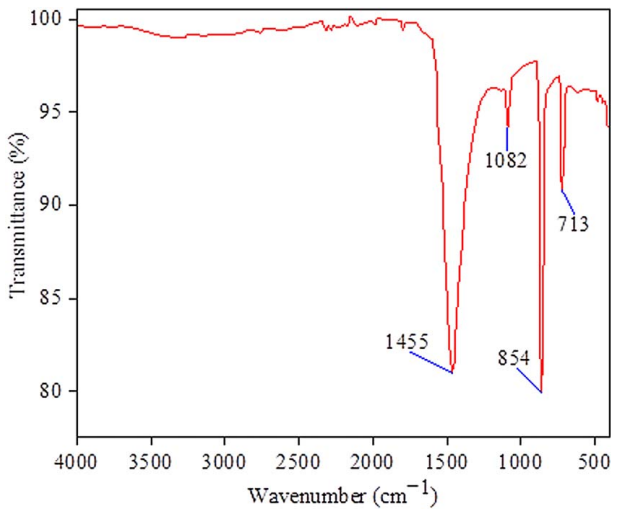

Fig. 5 FT-IR spectrum of unknown solid deposit sample E

Table 4 Experimental results for the elemental analysis of solid deposit sample E by MIP-AES

	Ca 643.907 nm		Ba 614.171 nm		Sr 650.399 nm		Na 568.263 nm		Fe 371.993 nm		Mg 518.360 nm		Cu 324.754 nm	
Solution	Conc	Int	Conc	Int	Conc	Int	Conc	Int	Conc	Int	Conc	Int	Conc	Int
Blank	0.00	0.00	0.00	0.00	0.00	0.00	0.00	0.00	0.00	0.00	0.00	0.00	0.00	0.00
Standard 1	0.50	509	0.50	9790	0.50	367	0.50	104	0.50	1223	0.50	2009	0.50	22,088
Standard 2	5.00	5021	5.00	207,571	5.00	3510	5.00	877	5.00	45,048	5.00	21,488	5.00	458,078
Standard 3	10.0	10,375	10.0	480,321	10.0	7572	10.0	1781	10.0	92,318	10.0	43,159	10.0	843,813
Standard 4	15.0	15,699	15.0	693,662	15.0	12,410	15.0	2973	15.0	144,753	15.0	68,705	15.0	1,263,162
Standard 5	20.0	21,486	20.0	945,627	20.0	16,112	20.0	3852	20.0	201,156	20.0	93,878	20.0	1,712,110
Standard 6	25.0	26,382	25.0	1,160,137	25.0	20,102	25.0	4895	25.0	254,858	25.0	122,504	25.0	2,099,917
Sample E	12.7	13,324	3.20	136,699	18.9	15,194	9.50	1816	2.60	21,553	3.00	12,490	11.8	996,814
SD	0.24	251.65	0.01	75.400	0.05	44.66	0.27	53.22	0.02	225.64	0.01	60.400	0.05	3989.47
RSD (%)	1.90	1.9100	0.32	0.0600	0.29	0.290	2.86	2.930	0.86	1.0500	0.42	0.4800	0.40	0.4000
ACESE	12.7 ± 0.24		3.2 ± 0.01		18.9 ± 0.05		9.5 ± 0.27		2.6 ± 0.02		3.0 ± 0.01		11.8 ± 0.05	
R^2	0.9997		0.9992		0.9987		0.9984		0.9986		0.9974		0.9994	

Note: Conc: concentration (ppm), Int: intensity (unitless), SD: standard deviation, RSD: relative standard deviation, ACESE: actual concentration of element in sample E (ppm), R^2: correlation coefficient, and nm: nanometer (SI unit of wavelength).

the unknown oilfield solid deposit sample E was calculated and the results obtained are tabulated in Table 5.

The results in Table 5 show that the concentration of Ca in unknown oilfield solid deposit sample E is much higher as compared with other elements. Therefore, this implies that the unknown oilfield solid deposit sample E was likely to be $CaCO_3$ scale as supported by the results obtained for XRD, TGA, and FT-IR. The percentage weight of the $CaCO_3$ scale in sample E from MIP-AES results was calculated based on the average percentage weight of Ca (33.6 wt%) with the aid of Eq. (7)

$$\underset{40.078\ \text{g/mol}}{Ca^{2+}(aq)} + \underset{60.01\ \text{g/mol}}{CO_3^{2-}(aq)} \rightleftharpoons \underset{100.09\ \text{g/mol}}{CaCO_3(s)} \quad (7)$$

The calculated percentage weight of the $CaCO_3$ scale in the unknown oilfield solid deposit sample E was found to be 83.9 wt %, this result is in good agreement with the results obtained from TGA analysis. A similar study was also done by Nelson et al. [43] on the trace elemental analysis of crude oils by using MIP-AES and reported that MIP-AES is the best technique for the trace elemental analysis in crude oil samples.

Calcium Carbonate Scale Removal. The unknown oilfield solid deposit sample E was identified as $CaCO_3$; thus, the acid treatment method that involves the use of HCl solution is the most appropriate and cost-effective [44]. $CaCO_3$ scale easily dissolves in hydrochloric acid solution producing water-soluble products which can be easily washed out by water (Eq. (8)) [2,45]

$$CaCO_3(s) + 2HCl(aq) \longrightarrow CaCl_2(aq) + CO_2(g) + H_2O(l) \quad (8)$$

The removal of the $CaCO_3$ scale by using HCl is the cheapest and easiest method to use especially when mechanical treatment methods are not applicable [13]. The disadvantage of this method is that HCl is highly corrosive, thus its application requires the addition of anticorrosive agents to the acid solution to reduce the corrosion effects [23]. The most recommended concentration of HCl solution for the removal of the $CaCO_3$ scale is 15% (by weight solution) [45]. The most important parameters to consider in acid treatments design include the amount of scale deposits in the oilfield system, concentration and volume of acid required, injection rate, and injection pressure [45]. The volume of HCl required to dissolve a given amount of $CaCO_3$ scale can be determined stoichiometrically with the aid of chemical reaction (Eq. (8)) by using Eq. (9) [45]

$$\alpha = C_a \frac{n_c \text{MW}_c}{n_a \text{MW}_a} \quad (9)$$

whereby α = gravimetric dissolving power of HCl solution, C_a = concentration of HCl solution (15%), n_c = number of mole of $CaCO_3$ scale (1 mol), n_a = number of mole of HCl (2 mol), MW_c = molecular weight of $CaCO_3$ scale (100.1 g/mol), and MW_a = molecular weight of HCl (36.5 g/mol).

Since the unknown oilfield solid deposit sample E was quantified by TGA and found to contain 89% of the $CaCO_3$ scale, the volume of 15% HCl solution required for its removal was calculated with the aid of Eq. (9). However, different volumes of 15% HCl solution were experimentally tested using a known amount of solid deposit sample E to determine the efficiency of 15% HCl solution in removing the solid deposit sample E as presented in Table 6.

The results shown in Table 6 were graphically presented as shown in Fig. 6 and it can be noted that 11 mL of 15% HCl solution was the maximum volume required to remove 3.001 g of solid deposit sample E. For the volumes of acid exceeding 11 mL, the efficiency does not change since the unknown solid deposit sample E contains only 89% as pure $CaCO_3$ plus other impurities which do not dissolve

Table 5 Results for the elemental analysis of unknown solid deposit sample E by MIP-AES

MSE (mg)	TVOS (mL)	ESE	MCE (ppm)	DF	CESE (ppm)	MESE (mg)	wt% of ESE
15.1	100	Ca	12.7 ± 0.24	4	50.8 ± 1.92	5.08 ± 0.192	33.6 ± 1.271
200	100	Ba	3.2 ± 0.01	1	3.2 ± 0.01	0.32 ± 0.002	0.16 ± 0.001
		Sr	18.9 ± 0.05	1	18.9 ± 0.05	1.89 ± 0.01	0.95 ± 0.005
		Na	9.5 ± 0.27	1	9.5 ± 0.27	0.95 ± 0.054	0.48 ± 0.027
		Fe	2.6 ± 0.02	1	2.6 ± 0.02	0.26 ± 0.004	0.13 ± 0.002
		Mg	3.0 ± 0.01	1	3.0 ± 0.01	0.30 ± 0.002	0.15 ± 0.001
		Cu	11.8 ± 0.05	1	11.8 ± 0.05	1.18 ± 0.01	0.59 ± 0.005

Note: CESE: concentration of element in sample E, MCE: measured concentration of element, DF: dilution factor, MESE: mass of element in sample E, TVOS: total volume of original solution, ESE: element in sample E, MSE: mass of sample E, and wt: weight.

Table 6 Experimental results on the efficiency of 15% HCl solution in removing the solid deposit sample E

	Mass of sample E used (3.001 g)							
Volume of HCl (mL)	1	3	5	7	9	11	13	15
Residual (g)	2.7519	2.2402	1.7636	1.2566	0.7523	0.3207	0.3206	0.3206
Mass change (g)	0.2491	0.7608	1.2374	1.7444	2.2487	2.6803	2.6804	2.6804
Efficiency (%)	8.3	25.4	41.2	58.1	74.9	89.3	89.3	89.3

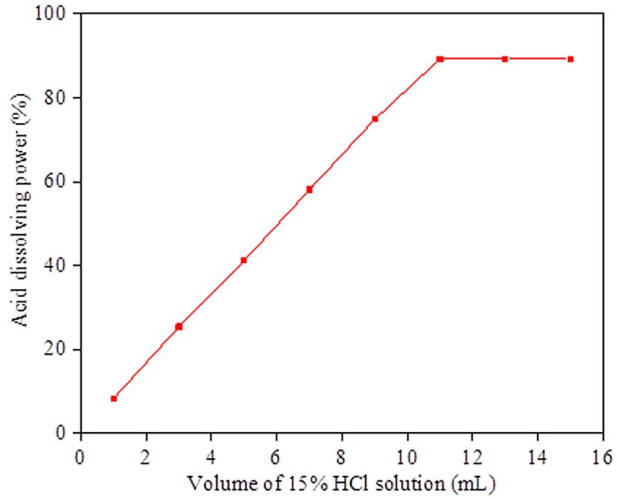

Fig. 6 A plot showing the efficiency of 15% HCl solution in removing a known amount of solid deposit sample E

15% HCl solution. From these results, it can be concluded that the exact amount of $CaCO_3$ scale deposit in the oilfield system, the concentration and volume of acid (HCl) solution needs to be accurately determined for the effective removal of $CaCO_3$ scale deposit. Nevertheless, the acid treatment methods should be carefully carried out with a clear understanding of the reservoir formations [46]. The reservoir formations may comprise bentonite, kaolinite, dolomite, siderite, quartz, sodium feldspar, and others [45]. These minerals can react with acids and results in reservoir formation damage if the acid treatment methods are not properly controlled.

Conclusion

In the present study, both qualitative and quantitative analyses were found very useful in the identification and quantification of the unknown oilfield solid deposit sample E. From the preliminary qualitative tests conducted, it was observed that the unknown oilfield solid deposit sample E was gray, insoluble (in water, toluene and n-hexane), and did not burn on flame, but it was soluble in 15% HCl. Based on the findings obtained from the preliminary qualitative tests and available instruments; XRD, TGA, FT-IR, and MIP-AES were chosen for the identification and quantification of unknown oilfield solid deposit sample E.

Through the experiments, it was confirmed that no individual technique can surely identify and quantify the unknown solid deposits from the oilfields. However, complete identification and quantification can only be achieved by combining information from both qualitative and quantitative analysis using several analytical techniques. In this study, XRD and FT-IR techniques were found very powerful in identifying the unknown oilfield solid deposit sample E, whereas TGA and MIP-AES were the most appropriate quantification techniques for the unknown oilfield solid deposit sample E.

The scaling problem for the oilfield where the unknown oilfield solid deposit sample E was collected is mainly due to the deposition of the $CaCO_3$ scale. The solid deposits due to the $CaCO_3$ scale in the oilfield systems can be effectively removed by using acid treatment methods such as HCl. The exact amount of $CaCO_3$ scale in the oilfield system, the concentration and volume of HCl solution required for the acid treatment method need to be accurately determined to ensure the effective removal of the $CaCO_3$ scale deposit in the oilfield system.

Acknowledgment

The authors would like to thank Dr. Andrew Kindness for the technical support during the laboratory experiments and Dr. Musa Mpelwa for proofreading this research paper.

Conflict of Interest

There are no conflicts of interest.

Data Availability Statement

The datasets generated and supporting the findings of this article are obtainable from the corresponding author upon reasonable request. The authors attest that all data for this study are included in the paper. No data, models, or code were generated or used for this paper.

Nomenclature

Å	=	Angstrom
Ba	=	barium
$BaSO_4$	=	barium sulfate
°C	=	degree celsius
Ca	=	calcium
C_a	=	concentration of acid (HCl)
$Ca(HCO_3)_2$	=	calcium bicarbonate
$CaCl_2$	=	calcium chloride
$CaCO_3$	=	calcium carbonate
CaO	=	calcium oxide
$CaSO_4$	=	calcium sulfate
cm	=	centimeter
CO_2	=	carbon dioxide
Cu	=	copper
$CuSO_4$	=	copper(II) sulfate
Fe	=	iron
$Fe(NO_3)_3$	=	iron(III) nitrate
$FeCO_3$	=	iron(II) carbonate
FeS	=	iron(II) sulfide
g	=	gram
g/mol	=	gram per mole
H_2CO_3	=	carbonic acid
H_2O	=	water
HCl	=	hydrochloric acid
HF	=	hydrofluoric acid
HNO_3	=	nitric acid
mg	=	milligram
Mg	=	magnesium
$MgCO_3$	=	magnesium carbonate

mL = milliliter
MW_a = molecular weight of acid (HCl)
MW_c = molecular weight of $CaCO_3$
n_a = number of mole of acid (HCl)
Na = sodium
Na_2SO_4 = sodium sulfate
n_c = number of mole of $CaCO_3$
ppm = parts per million
Sr = strontium
$Sr(NO_3)_2$ = strontium nitrate
$SrSO_4$ = strontium sulfate
Std = standard
wt = weight
α = acid dissolving power
θ = diffraction angle

References

[1] Gonzalez, D. L., Jamaluddin, A. K. M., Solbakken, T., Hirasaki, G. J., and Chapman, W. G., 2007, "Impact of Flow Assurance in the Development of a Deepwater Prospect," Paper Presented at the SPE Annual Technical Conference and Exhibition, Anaheim, CA., November, Vol. 6, pp. 3883–3892.
[2] Olajire, A. A., 2015, "A Review of Oilfield Scale Management Technology for Oil and Gas Production," J. Pet. Sci. Eng., **135**, pp. 723–737.
[3] Jamaluddin, A. K. M., Nighswander, J., and Joshi, N., 2003, "A Systematic Approach for Characterizing Hydrocarbon Solids," SPE J., **8**(3), pp. 304–312.
[4] Moghadasi, J., Jamialahmadi, M., Müller-Steinhagen, H., and Sharif, A., 2004, "Formation Damage Due to Scale Formation in Porous Media Resulting From Water Injection," Paper Presented at the SPE International Symposium and Exhibition on Formation Damage Control, Lafayette, LA, February, pp. 581–591.
[5] Sadeq, D., Iglauer, S., Lebedev, M., Smith, C., and Barifcani, A., 2017, "Experimental Determination of Hydrate Phase Equilibrium for Different Gas Mixtures Containing Methane, Carbon Dioxide and Nitrogen With Motor Current Measurements," J. Nat. Gas Sci. Eng., **38**, pp. 59–73.
[6] Scott, S. L., and Yi, J., 1999, "Flow Testing Methods to Detect and Characterize Partial Blockages in Looped Subsea Flowlines," ASME J. Energy Resour. Technol., **121**(3), pp. 154–160.
[7] BinMerdhah, A. B., Yassin, A. A. M., and Muherei, M. A., 2010, "Laboratory and Prediction of Barium Sulfate Scaling at High-Barium Formation Water," J. Pet. Sci. Eng., **70**(1–2), pp. 79–88.
[8] Struchkov, I. A., Rogachev, M. K., Kalinin, E. S., Pavlov, P. V., and Roschin, P. V., 2018, "Laboratory Investigation of Organic-Scale Prevention in a Russian Oil Field," SPE Prod. Oper., **33**(1), pp. 113–120.
[9] Mpelwa, M., and Tang, S. F., 2019, "State of the Art of Synthetic Threshold Scale Inhibitors for Mineral Scaling in the Petroleum Industry: A Review," Pet. Sci., **16**(4), pp. 113–120.
[10] Gupta, A., and Anirbid, S., 2015, "Need of Flow Assurance for Crude Oil Pipelines: A Review," Int. J. Multidiscip. Sci. Eng., **6**(2), pp. 43–49.
[11] Vazirian, M. M., Charpentier, T. V. J., de Oliveira Penna, M., and Neville, A., 2016, "Surface Inorganic Scale Formation in Oil and Gas Industry: As Adhesion and Deposition Processes," J. Pet. Sci. Eng., **137**, pp. 22–32.
[12] Liu, X., Jungang, L., Qianya, Z., Jinlai, F., Yingli, L., and Jingxin, S., 2009, "The Analysis and Prediction of Scale Accumulation for Water-Injection Pipelines in the Daqing Oilfield," J. Pet. Sci. Eng., **66**(3–4), pp. 161–164.
[13] Kamal, M. S., Hussein, I., Mahmoud, M., Sultan, A. S., and Saad, M. A. S., 2018, "Oilfield Scale Formation and Chemical Removal: A Review," J. Pet. Sci. Eng., **171**, pp. 127–139.
[14] Sanni, O., Kapur, N., Charpentier, T., and Neville, A., 2015, "Study of Surface Deposition and Bulk Scaling Kinetics in Oilfield Conditions Using an In-Situ Flow Rig," NACE—International Corrosion Conference Series, Dallas, TX, pp. 1–15.
[15] Theyab, M. A., and Yahya, S. Y., 2018, "Introduction to Wax Deposition," Int. J. Petrochemistry Res., **2**(1), pp. 126–131.
[16] Ellison, B. T., Gallagher, C. T., and Lorimer, S. E., 2000, "The Physical Chemistry of Wax, Hydrates, and Asphaltene," SPE Repr. Ser., **58**, pp. 133–143.
[17] Toma, P., Ivory, J., Korpany, G., DeRocco, M., Holloway, L., Goss, C., Ibrahim, J., and Omar, I., 2006, "A Two-Layer Paraffin Deposition Structure Observed and Used to Explain the Removal and Aging of Paraffin Deposits in Wells and Pipelines," ASME J. Energy Resour. Technol., **128**(1), pp. 49–61.
[18] Theyab, M. A., 2018, "Fluid Flow Assurance Issues: Literature Review," SciFed J. Pet., **2**(1), pp. 1–11.
[19] Alharooni, K., Barifcani, A., Pack, D., Gubner, R., and Ghodkay, V., 2015, "Inhibition Effects of Thermally Degraded MEG on Hydrate Formation for Gas Systems," J. Pet. Sci. Eng., **135**, pp. 608–617.
[20] Uddin, M., Coombe, D., Law, D., and Gunter, B., 2008, "Numerical Studies of Gas Hydrate Formation and Decomposition in a Geological Reservoir," ASME J. Energy Resour. Technol., **130**(3), p. 032501.
[21] Hammami, A., and Ratulowski, J., 2007, "Precipitation and Deposition of Asphaltenes in Production Systems: A Flow Assurance Overview," Asph. Heavy Oils, Pet., pp. 617–660.
[22] Dahaghi, A. K., Gholami, V., and Moghadasi, J., 2008, "Formation Damage Through Asphaltene Precipitation Resulting From CO_2 Gas Injection in Iranian Carbonate Reservoirs," SPE Prod. Oper., pp. 210–214.
[23] Merdhah, A. B., 2007, "Study of Scale Formation in Oil Reservoir During Water Injection—A Review," Mar. Sci. Technology Semin., pp. 1–189.
[24] Mackay, E. J., and Jordan, M. M., 2005, "Impact of Brine Flow and Mixing in the Reservoir on Scale Control Risk Assessment and Subsurface Treatment Options: Case Histories," ASME J. Energy Resour. Technol., **127**(3), pp. 201–213.
[25] Kamari, A., Gharagheizi, F., Bahadori, A., and Mohammadi, A. H., 2014, "Determination of the Equilibrated Calcium Carbonate (Calcite) Scaling in Aqueous Phase Using a Reliable Approach," J. Taiwan Inst. Chem. Eng., **45**(4), pp. 1307–1313.
[26] El-Said, M., Ramzi, M., and Abdel-Moghny, T., 2009, "Analysis of Oilfield Waters by Ion Chromatography to Determine the Composition of Scale Deposition," Desalination, **249**(2), pp. 748–756.
[27] Itoro, O., Sylvester, O., and Appah, D., 2015, "Barium Sulphate Scaling Prevention," Int. J. Eng. Technol., **5**(4), pp. 254–263.
[28] Cosultchi, A., Garciafigueroa, E., Mar, B., García-Bórquez, A., Lara, V. H., and Bosch, P., 2002, "Contribution of Organic and Mineral Compounds to the Formation of Solid Deposits Inside Petroleum Wells," Fuel, **81**(4), pp. 413–421.
[29] Crabtree, M., Eslinger, D., Fletcher, P., Miller, M., Johnson, A., and King, G., 1999, "Fighting Scale—Removal and Prevention," Oilf. Rev., pp. 30–45.
[30] Kang, P. S., Hwang, J. Y., and Lim, J. S., 2019, "Flow Rate Effect on Wax Deposition Behavior in Single-Phase Laminar Flow," ASME J. Energy Resour. Technol., **141**(3), p. 032903.
[31] Bui, T. D., 2015, Preventing Oil Spills Caused by Gas Hydrates, http://www.archer.ac.uk/casestudies/Archer_gas_casestudy.pdf, Accessed October 10, 2019.
[32] Doelman, J. D. B., 2013, Control Scale to Optimize HVAC Equipment Energy Efficiency, https://www.fmamfg.org/blog/control-scale-optimize-hvac-equipment-energy-efficiency, Accessed October 1, 2019.
[33] Lai, N., Wen, Y., Wang, Y., Zhao, X., Chen, J., Wang, D., Wang, X., Yu, T., and Jia, C., 2020, "Calcium Carbonate Scaling Kinetics in Oilfield Gathering Pipelines by Using a 1D Axial Dispersion Model," J. Pet. Sci. Eng., **188**, p. 106925.
[34] Marfo, S. A., Opoku Appau, P., and Kpami, L. A. A., 2018, "Subsea Pipeline Design for Natural Gas Transportation: A Case Study of Côte D'ivoire's Gazelle Field," Int. J. Pet. Petrochemical Eng., **4**(3), pp. 21–34.
[35] Ilevtifieieva, O. A., Bolotov, V. V., Kostina, T. A., Svechnikova, O. M., Yuschenko, T. I., Kaminska, N. I., Kosareva, A. E., Slobodyanyuk, L. V., and Yashchuk, O. P., 2014, *Analytical Chemistry (Qualitative Analysis) Part I the Manual for Students of Higher Schools*.
[36] Ang, H. H., and Lee, K. L., 2005, "Analysis of Mercury in Malaysian Herbal Preparations," J. Med. Biomed. Res., **4**(1), pp. 31–36.
[37] Xu, B., and Poduska, K. M., 2014, "Linking Crystal Structure With Temperature-Sensitive Vibrational Modes in Calcium Carbonate Minerals," Phys. Chem. Chem. Phys., **16**(33), pp. 17634–17639.
[38] Sarkar, A., and Mahapatra, S., 2012, "Mechanism of Unusual Polymorph Transformations in Calcium Carbonate: Dissolution-Recrystallization vs Additive-Mediated Nucleation," J. Chem. Sci., **124**(6), pp. 1399–1404.
[39] Kodel, K. A., Andrade, P. F., Valença, J. V. B., and Souza, D. D. N., 2012, "Study on the Composition of Mineral Scales in Oil Wells," J. Pet. Sci. Eng., **81**, pp. 1–6.
[40] Xyla, A. G., and Koutsoukos, P. G., 1989, "Quantitative Analysis of Calcium Carbonate Polymorphs by Infrared Spectroscopy," J. Chem. Soc. Faraday Trans. 1 Phys. Chem. Condens. Phases, **85**(10), pp. 3165–3172.
[41] Poirier, L., Nelson, J., Gilleland, G., Wall, S., Berhane, L., and Lopez-Linares, F., 2017, "Comparison of Preparation Methods for the Determination of Metals in Petroleum Fractions (1000°F+) by Microwave Plasma Atomic Emission Spectroscopy," Energy Fuels, **31**(8), pp. 7809–7815.
[42] Nelson, J., Gilleland, G., Poirier, L., Leong, D., and Hajdu, P., 2016, *Direct Multi-Elemental Analysis of Crude Oils Using the Agilent 4200/4210 Microwave Plasma-Atomic Emission Spectrometer Application Note Authors*, Agilent Technologies, Inc., Santa Clara, CA, pp. 135–139.
[43] Nelson, J., Gilleland, G., Poirier, L., Leong, D., Hajdu, P., and Lopez-Linares, F., 2015, "Elemental Analysis of Crude Oils Using Microwave Plasma Atomic Emission Spectroscopy," Energy Fuels, **29**(9), pp. 5587–5594.
[44] Eltaib, O. E., and Rabah, A. A., 2012, "Crude Oil Pipeline Scale Deposition: Causes and Removal Methods," Annual Conference of Postgraduate Studies and Scientific Research, Vol. 2: Engineering, University of Khartoum Engineering Journal, Sudan, pp. 1–6.
[45] Guo, B., Liu, X., and Tan, X., 2017, *"Acidizing," Petroleum Production Engineering*, Gulf Professional Publishing, Oxford, UK, pp. 367–387.
[46] Azeta, G., Joel, O., and Kinigoma, A., 2012, "Identification of Formation Scale and Modeling of Treatment Fluid," Res. J. Eng. Sci., **1**(3), pp. 5–10.